

# UC Davis

## San Francisco Estuary and Watershed Science

### Title

Investigating Particle Transport and Fate in the Sacramento–San Joaquin Delta Using a Particle-Tracking Model

### Permalink

<https://escholarship.org/uc/item/547917qn>

### Journal

San Francisco Estuary and Watershed Science, 6(1)

### Authors

Kimmerer, Wim J.  
Nobriga, Matthew L.

### Publication Date

2008

### DOI

<https://doi.org/10.15447/sfew.2008v6iss1art4>

### Copyright Information

Copyright 2008 by the author(s). This work is made available under the terms of a Creative Commons Attribution License, available at <https://creativecommons.org/licenses/by/4.0/>

Peer reviewed

# Investigating Particle Transport and Fate in the Sacramento-San Joaquin Delta Using a Particle Tracking Model

Wim J. Kimmerer, San Francisco State University\*  
Matthew L. Nobriga, CALFED Science Program

\*Corresponding author: [kimmerer@sfsu.edu](mailto:kimmerer@sfsu.edu)

## ABSTRACT

Movements of pelagic organisms in the tidal freshwater regions of estuaries are sensitive to the movements of water. In the Sacramento-San Joaquin Delta—the tidal freshwater reach of the San Francisco Estuary—such movements are key to losses of fish and other organisms to entrainment in large water-export facilities. We used the Delta Simulation Model-2 hydrodynamic model and its particle tracking model to examine the principal determinants of entrainment losses to the export facilities and how movement of fish through the Delta may be influenced by flow. We modeled 936 scenarios for 74 different conditions of flow, diversions, tides, and removable barriers to address seven questions regarding hydrodynamics and entrainment risk in the Delta. Tide had relatively small effects on fate and residence time of particles. Release location and hydrology interacted to control particle fate and residence time. The ratio of flow into the export facilities to freshwater flow into the Delta (export:inflow or EI ratio) was a useful predictor of entrainment probability if the model were allowed to run long enough to resolve particles' ultimate fate. Agricultural diversions within

the Delta increased total entrainment losses and altered local movement patterns. Removable barriers in channels of the southern Delta and gates in the Delta Cross Channel in the northern Delta had minor effects on particles released in the rivers above these channels. A simulation of losses of larval delta smelt showed substantial cumulative losses depending on both inflow and export flow. A simulation mimicking mark-recapture experiments on Chinook salmon smolts suggested that both inflow and export flow may be important factors determining survival of salmon in the upper estuary. To the extent that fish behave passively, this model is probably suitable for describing Delta-wide movement, but it is less suitable for smaller scales or alternative configurations of the Delta.

## KEYWORDS

tidal processes, water diversions, particle tracking model, San Francisco Estuary, Chinook salmon *Oncorhynchus tshawytscha*, delta smelt *Hypomesus transpacificus*

## SUGGESTED CITATION

Kimmerer, Wim J.; Matthew L. Nobriga. 2008. Investigating Particle Transport and Fate in the Sacramento-San Joaquin Delta Using a Particle Tracking Model. *San Francisco Estuary and Watershed Science*, Vol. 6, Issue 1 (February), Article 4.

## INTRODUCTION

In tidal river estuaries, freshwater flows affect hydrodynamic phenomena important to biotic communities. Examples include the geographic match or mismatch of chemically and structurally appropriate habitat attributes (Peterson 2003), strength of entrainment phenomena such as gravitational circulation and residual landward bottom currents that concentrate biota and assist retention in rearing habitats (Cronin and Forward 1979; Kimmerer et al. 2002), and flow pulses that transport larvae to rearing habitats (Dew and Hecht 1994). Thus, freshwater depletions and changes in the timing of freshwater inputs affect estuarine biota, often negatively (Jassby et al. 1995; Livingston et al. 1997).

The landward reach of California's San Francisco Estuary, known as the Sacramento-San Joaquin Delta, may be the only place in the world where significant freshwater is diverted from within a tidal estuary. Reservoir releases throughout the watershed are managed to maintain most of the Delta as a permanently freshwater ecosystem to support a significant redistribution of California's water resources from north to south (Kimmerer 2002). Four large water diversions owned by the U.S. and State of California governments collectively export an average of nearly 7 cubic kilometers per year ( $\text{km}^3 \text{ yr}^{-1}$ ) from the Delta (Table 1). More than 95% of the water exported from the Delta is taken by the two largest diversions: the Jones Pumping Plant of the federal Central Valley Project (hereafter, CVP) and the State Water Project's Banks Pumping Plant (hereafter, SWP). Existing regulations allow for up to 65% of river inflows to be diverted during certain months. The exported water is pumped to agricultural, municipal, and industrial users to the south and west; an estimated 22 million Californians use water exported from the Delta.

In addition to the water exported out of the Delta, an estimated net  $0.1 \text{ km}^3 \text{ yr}^{-1}$  also is removed during April–September to irrigate farmlands within the Delta (Brown 1982). The within-Delta farmlands are irrigated by approximately 2,200 comparatively small, privately-owned water diversions scattered throughout the system (Herren and Kawasaki 2001).

Numerous fish species migrate through or live in the upper San Francisco Estuary during all or part of their life cycles (Moyle 2002). Thus, in addition to altered hydrodynamics, the large-scale removal of freshwater from the Delta adds the potential for significant entrainment of fishes from the upper estuary. Entrainment of the early life stages of fish has been a long-standing concern (Stevens et al. 1985; Moyle et al. 1992; Brandes and McLain 2001). Elaborate facilities operate continuously at each export plant to separate fish from diverted water and return them to the estuary (Brown et al. 1996). Although mortality of some species at these facilities is probably high (e.g., Bennett 2005), correlative evidence of major entrainment effects on fish population dynamics has not been forthcoming (Kimmerer et al. 2001; Newman 2003; Bennett 2005).

A quantitative understanding of linkages between Delta hydrodynamics and fish entrainment risk has been hindered by difficulties in modeling the Delta's complex network of tidally-influenced channels, incremental changes in SWP and CVP water opera-

**Table 1.** Summary of annual export volumes ( $\text{km}^3$ ) from the four state and federal water diversions in the Sacramento-San Joaquin Delta for water years following the Bay-Delta Accord (1995–2005). The Contra Costa and Tracy diversion facilities are part of the federal Central Valley Project. The Harvey O. Banks and North Bay Aqueduct diversion facilities are part of the State Water Project.

Water Diversion	1st Year of Operation	Average Volume (range)
Contra Costa	1940	0.15 (0.12 – 0.23)
Tracy (CVP)	1951	3.1 (2.6 – 3.5)
Banks (SWP)	1968	3.6 (2.1 – 4.9)
North Bay Aqueduct	1988	0.05 (0.03 – 0.07)

tions, and the large natural inter-annual and seasonal variability in inflow. During the latter half of the twentieth century, the number of water diversions increased (Table 1), as did total water export volumes (Kimmerer 2002). Furthermore, the number of flow control structures, such as barriers and flood gates, has increased and their operation schedules have changed through time. Proposals for further modifications continue.

We used the Delta Simulation Model-2 hydrodynamic model (DSM2 HYDRO) and its associated particle tracking model (PTM) to examine the principal determinants of entrainment losses to the export facilities, under assumptions discussed below. We explored numerous combinations of freshwater inflow, export flow, and tide for a variety of particle release sites. Our goal was to provide information about Delta hydrodynamics, water diversions, and barrier operations pertinent to management of the Delta for fish. We addressed the following questions regarding hydrodynamics and entrainment risk in the Delta: (1) What effect do spring versus neap tides have on particle fate? (2) How do release location, hydrology, and time interact to influence particle fates? (3) What is the best index of export flows in the Delta to index the probability of entrainment of neutrally-buoyant particles and (possibly) resident and migratory fish? (4) What is the effect of in-Delta agricultural diversions on entrainment loss and particle residence time? (5) What is the effect of permanent and temporary barriers on entrainment loss and particle residence time? (6) How can the entrainment of the larvae of threatened delta smelt (*Hypomesus transpacificus*) be related to hydrodynamic conditions? (7) How do freshwater inflow and export flow affect the predicted passage out of the Delta of particles released at sites in the northern Delta where Chinook salmon (*Oncorhynchus tshawytscha*) smolts are released for experiments on survival?

## METHODS

### Study Area

Numerous alterations of the Sacramento-San Joaquin Delta influence hydrodynamics and the movement of fish in the system (Figure 1). For example, the Yolo

Bypass, an artificial floodplain of the Sacramento River, is managed to take most of the winter flood flows and prevent flooding of urban areas (Sommer et al. 2001). The Delta Cross Channel (DCC) connects the Sacramento River with the interior Delta by way of a pair of movable gates, which are closed during floods and when salmon are migrating downstream. Temporary rock barriers are installed at various sites in the southern Delta to maintain water levels for agricultural diversions, and one barrier is placed at the head of Old River to prevent salmon smolts from entering it during their migration down the adjoining San Joaquin River. One objective of closing the DCC and the barrier at the head of Old River is to minimize salmon losses that can be attributed to water project operations.

### Hydrodynamic Model

DSM2 HYDRO is a one-dimensional (1-D) numerical model that simulates non-steady state hydrodynamics in a network of riverine and estuarine channels using a standard numerical method (the Preissman scheme). (See <http://baydeltaoffice.water.ca.gov/modeling/deltamodeling/>). The chief advantages of this model are its speed, and the fact that the California Department of Water Resources (CDWR) has expended a tremendous amount of effort and care in developing, calibrating, and testing this model. The model grid consists of 416 nodes and 509 links representing channels, and open-water areas, which are represented as reservoirs where mixing occurs. Seventeen hydraulic barriers and gates are also included. DSM2 HYDRO's primary dependent variables are stage and flow; the model boundary conditions are stage at Martinez to the west, water diversions in the Delta, and stream flows at the landward limits of tidal influence. DSM2 HYDRO was calibrated to empirical flow and stage data (May 1988, April 1997, April 1998, September–October 1998; CDWR 2001). The model's friction parameters for each of ~50 regions were adjusted until simulated values best matched observed daily average and instantaneous flow and stage data. The model calibration was validated by comparing simulated flow and stage with field data from 1990–1999. Results of this calibration and validation are available in the form of maps with select-

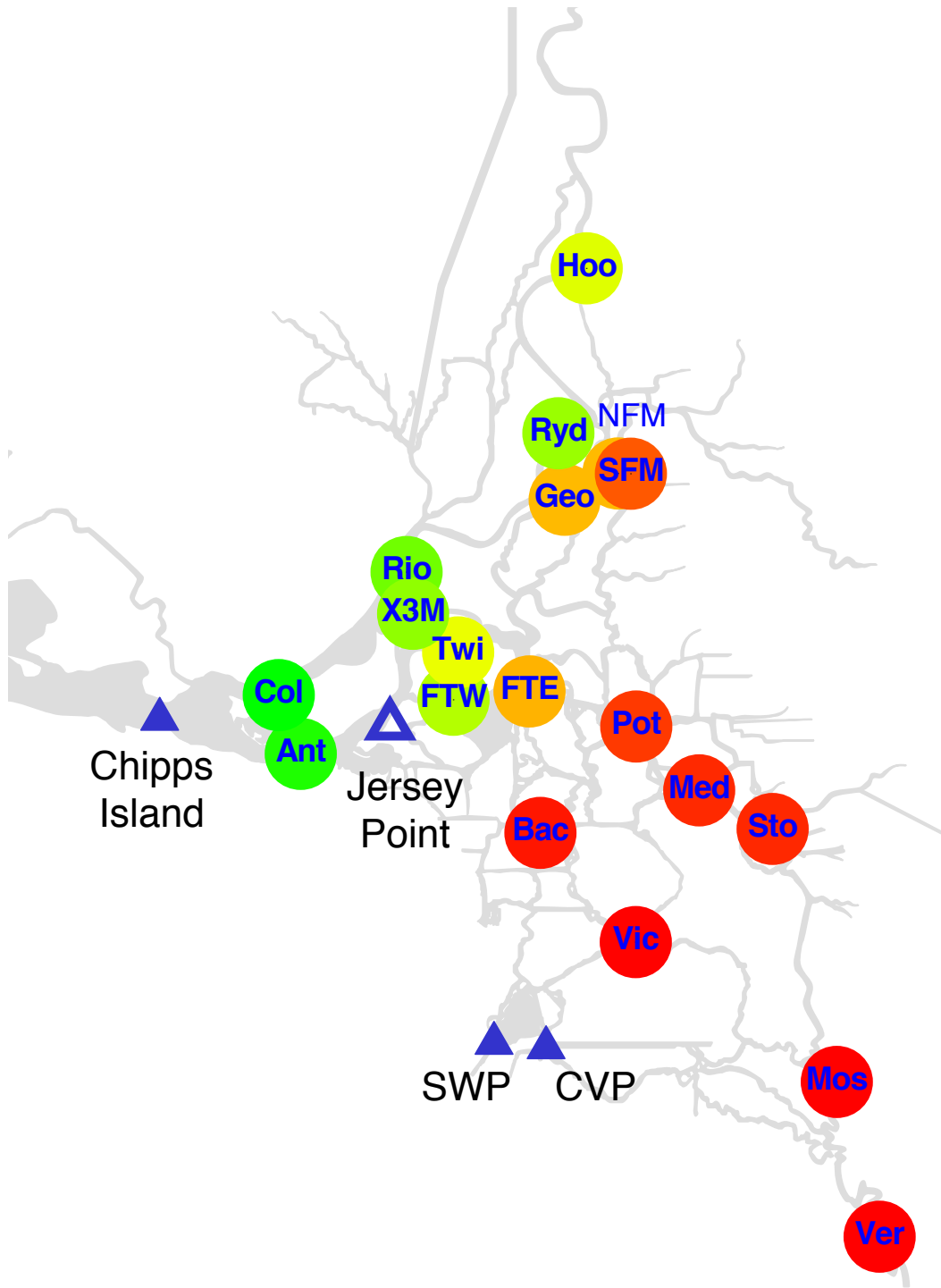


**Figure 1.** Map of the Sacramento-San Joaquin Delta showing release sites used in the particle tracking model. Sites are identified by codes listed in Table 4, and color-coded by the mean losses from each site to the SWP and CVP pumps. Blue triangles identify additional locations where particle passage was recorded: Chipps Island in the western Delta, and the federal and state water export facilities. The open triangle denotes an intermediate passage location at Jersey Point; others are at Georgiana Slough (Geo), the nearby DCC (not shown on map), and Rio Vista (Rio). The NFM site is covered by the SFM symbol. The Sac site is just north of the area shown on the map.

able nodes that link to graphical displays of model results and data (see <http://baydeltaoffice.water.ca.gov/modeling/deltamodeling/dsm2studies.cfm>).

DSM2 QUAL is a transport module that has been similarly calibrated against conductivity measurements at various Delta locations. This provides some assurance that the movement of substances, and therefore also neutrally-buoyant particles, is accurately represented, since both models use the same hydrodynamic output. However, PTM (see below) uses a very different scheme for velocity profiles and for mixing at junctions. Furthermore, model accuracy varies depending on the length of the simulation and the location of particle releases. The most recent calibration is available, also in the form of graphical displays, at <http://modeling.water.ca.gov/Delta/studies/calibration2000/>.

The DSM2 particle tracking model (PTM) is a quasi-3-D extension of DSM2 HYDRO (Culberson et al. 2004). The PTM represents movement of particles through advection in the mean flow together with a synthetic dispersion (Wilbur 2000; 2001). Each particle has a random component of movement—a random walk (Visser 1997)—and its position in the channel is tracked. Lateral velocity profiles are assumed to have a fourth-order polynomial description, and vertical profiles are logarithmic. Thus, particles may encounter velocities that differ substantially from the mean flow. These profiles are the same for all channels and therefore do not take into account channel shapes, nor do they make use of the change in vertical profiles that should accompany the bottom friction coefficients used to tune the hydrodynamic model. The combination of random movement and velocity shear results in dispersion of particles. However, upon reaching a junction or an open-water area, a particle is completely and instantaneously mixed, destroying information about its previous relative position in the channel. This is likely to have a significant effect on dispersion but this cannot be determined without re-coding the PTM. Velocity profiles used in the PTM were determined by fitting the profiles to velocity data collected at 16 sites in the Delta (Oltmann 1998; Wilbur 2000). The simulated quasi-3-D profiles were checked using simulations of dye concentration data collected from three stations following a single dye

release on the San Joaquin River; arrival time was reproduced well, but dispersion was less well predicted (Wilbur 2000).

Despite the extensive use of the DSM2 family of models to solve important management problems in the Delta, the calibrations and validations described above do not provide sufficient information for users to assess the accuracy or reliability of model output. There is no published record of the overall statistical properties of the models. To avoid relying on such uncertain foundations, we have conducted a partial analysis of the statistical properties of HYDRO and QUAL in relation to field data, and present our findings in the Appendix. This analysis is quite encouraging about the utility of these modules for the analysis of movements of water and salt on the scale of the Delta. However, we have not evaluated the extent to which the PTM reliably records the movement of particles. The comparisons with field data described above do not constitute a sufficient calibration of PTM. This shortfall could be addressed indirectly through a comparison of particle releases in PTM with tracer releases in QUAL, but that is beyond our scope. Furthermore, the basic formulation of the PTM has not been subjected to peer review.

Although the DSM2 models are simpler than others in use in this and other estuaries, the number of different dimensions of a modeling problem can become unwieldy even with this model. We chose to simplify the analysis by our choices of conditions to model, and our approach to the analysis. We used synthetic hydrology and repeating tides, which were either spring tides or, in a few runs, neap tides. We focused on spring tides to maximize dispersion effects, which appeared to be small (see Results). Inflows and export flows were constant during each model run, and distributed among the various sources and sinks based on historical data from the DAYFLOW accounting program for 1980–2002 (<http://www.iep.ca.gov/dayflow/>). Inflow was distributed by a constant proportion, except for the Yolo Bypass, which flows only under flood conditions (Table 2). Export flow was constant for the North Bay Aqueduct ( $0.9 \text{ m}^3 \text{ s}^{-1}$ ) and Contra Costa Canal ( $0.09 \text{ m}^3 \text{ s}^{-1}$ ), and the remainder was apportioned between the CVP and SWP (Table 2). Agricultural diversions were set to winter values



**Table 2.** Distributions of inflow and export flow by source for each model run.

Inflow		Inflow by Source (m <sup>3</sup> s <sup>-1</sup> )			
cfs	m <sup>3</sup> s <sup>-1</sup>	Sacramento R.	Yolo Bypass	San Joaquin R.	Eastern Delta
12,000	340	292	0	40	8
21,000	595	493	6	78	18
38,000	1,077	837	32	162	47
67,000	1,899	1,331	158	306	104
120,000	3,401	1,844	802	547	208

Export Flow		Export Flow by Source (m <sup>3</sup> s <sup>-1</sup> )			
cfs	m <sup>3</sup> s <sup>-1</sup>	SWP	CVP	Contra Costa Canal	North Bay Aqueduct
2,000	57	20	37	0.09	0.9
6,000	170	92	78	0.09	0.9
10,000	284	164	120	0.09	0.9

**Table 3.** Summary of model runs. Base runs were conducted with no agricultural diversions, south Delta barriers removed, and Delta Cross Channel (DCC) closed only for inflow greater than 38,000 cfs. “All” includes base runs, runs with agricultural diversions, releases from the north Delta with the DCC closed, and releases from Vernalis and Mossdale with various barrier configurations. In the lower part of the table, “Tide” refers to releases from all sites with neap and spring tides, “Ag Barriers” to releases from many sites with agricultural and fish barriers in place, and “Replicates” to multiple releases from the Hood site on the Sacramento River to test variability with different random number seeds.

Inflow		Export Flow									
cfs	m <sup>3</sup> s <sup>-1</sup>	Cfs m <sup>3</sup> s <sup>-1</sup>	2,000 57	5,000 142	6,000 170	7,000 198	8,000 227	9,000 255	10,000 283	11,000 312	12,000 340
12,000	340	All	Base	All	Base	Base	Base	Base	All		
21,000	595	All		All	Base	Base	Base	Base	All	Base	Base
38,000	1,077	Base		Base					Base		
67,000	1,899	Base		Base					Base		
120,000	3,401	Base		Base					Base		
12,000	340	Tide Replicates Ag Barriers		Ag Barriers					Tide Replicates		
38,000	1,077			Replicates							
120,000	3,401	Tide		Replicates					Tide		

( $0.9 \text{ m}^3 \text{ s}^{-1}$ ), except for a subset of runs in which they were set to typical summer values ( $127 \text{ m}^3 \text{ s}^{-1}$ ). Our use of minimum agricultural diversion demand in most runs reduced particle losses to agricultural diversions to  $< 1\%$  in all runs. This maximized the numbers of particles that remained in Delta channels for evaluation of study questions not involving these diversions. This choice was motivated by recent studies that suggest fish losses to small diversions are likely much less than expected based on quantities diverted (Nobriga et al. 2004; Moyle and Israel 2005). In most runs, temporary barriers in the south Delta were absent, and the Delta Cross Channel gates were open at inflow below  $600 \text{ m}^3 \text{ s}^{-1}$  and closed above, except in specific runs. These choices somewhat limit the interpretation of our results, but even so we modeled 936 scenarios for 74 different conditions of flow, diversions, tides, and barriers (Table 3, Figure 2).

## Data Analysis

For each model run, 4,000–5,000 particles were released at one of up to 20 sites (Table 4; Figure 1). Four to five thousand was approximately the maximum number of particles for which all particle fluxes could be calculated for a 90-day simulation. We always tried 5,000 particles first. If all particle fates could not be calculated, we re-ran the simulation using 4,000 particles. Equal numbers of particles were released at 15-minute intervals over the first 25 hours of each simulation to eliminate bias due to releasing particles on a particular tidal stage (Culberson et al. 2004). Model outputs consisted of hourly cumulative proportions of particles that passed selected control points (Figure 1). Except for analysis of tidal effects, data were filtered with a Godin low-pass filter (24 hours) and averaged over each day. Data at the beginning of the series were replaced by a straight daily average since the tidal filter removes the first 24 data points. Daily averages were then truncated to 90 days for all analyses.

Particles were considered to have left the Delta if they passed Chipps Island (Figure 1) or entered either the SWP or CVP pumping plants or agricultural diversions. Intermediate points were used only to assess the pathways that the particles had taken.

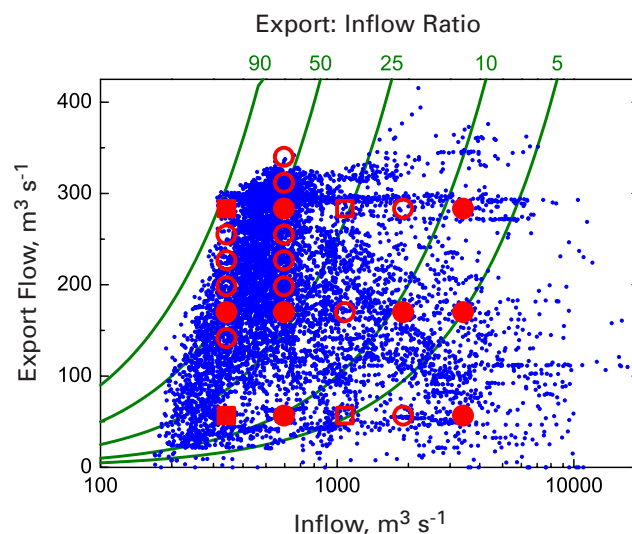


**Figure 2.** Daily export flow and inflow from the Dayflow accounting program for 1980–2002 (blue symbols) and values used in the model (red). Open symbols are base run only, filled symbols are other runs as described in Table 3. Squares are combinations used in examples (Figures 5 and 6). Green lines give isopleths of export:inflow (EI) ratio.

Generally, the profile of particle passage was asymmetrically sigmoid, with a rapid initial increase in slope followed by a protracted approach to an asymptote. For some release sites, particularly those in the southeastern Delta, there were two inflections in the recovery curves, as the particles took a shorter and a longer path to the recovery site. In a few cases, particles were still accumulating at endpoints at an accelerating rate at the end of the model run.

In many runs, particularly those at low flow for release points in the central and southern Delta, a substantial fraction of the particles remained in the Delta after 90 days. To estimate the ultimate fate of these particles, we extrapolated the curves of cumulative passage to infinite time. This extrapolation used a negative exponential curve fitted to the data past the last inflection point. The inflection point was determined by smoothing the curve with a 9-day running mean, and determining the locations of peaks in the data after differencing, i.e., subtracting each value from the previous value. The last peak in the differenced series was taken as the point of the final inflection. If there were no inflection, the



**Table 4.** Release and recovery points and codes used in the figures.

Release Site	River	Code	DSM2 Node	Study Questions
Vernalis	San Joaquin	Ver	1	1, 2, 3, 4, 5
Mossdale	San Joaquin	Mos	7	1, 2, 3, 4, 5
Stockton	San Joaquin	Sto	21	1, 2, 3, 4, 5, 6
Medford Island	San Joaquin	Med	25	1, 2, 3, 4, 5, 6
Potato Slough	San Joaquin	Pot	32	1, 2, 3, 4, 5, 6
Twitchell Island	San Joaquin	Tw	42	1, 2, 3, 4, 5, 6
Antioch	San Joaquin	Ant	46	1, 2, 3, 4, 5, 6
Bacon Island	Old	Bac	92	1, 2, 3, 4, 5, 6
Frank’s Tract East	n/a	FTE	103	1, 2, 3, 4, 5, 6
Frank’s Tract West	n/a	FTW	226	1, 2, 3, 4, 5, 6
Victoria Canal	Middle	Vic	113	1, 2, 3, 4, 5, 6
Three-Mile Slough	n/a	X3M	240	1, 2, 3, 4, 5, 6
South Fork Mokelumne	Mokelumne	SFM	261	1, 2, 3, 4, 6
North Fork Mokelumne	Mokelumne	NFM	281	1, 2, 3, 4
Georgiana Slough		Geo	291	1, 2, 3, 4, 5, 7
Sacramento	Sacramento	Sac	330	7
Hood	Sacramento	Hoo	338	1, 2, 3, 4, 5, 7
Ryde	Sacramento	Ryd	344	1, 2, 3, 4, 5, 7
Rio Vista	Sacramento	Rio	351	1, 2, 3, 4, 6
Collinsville	Sacramento	Col	354	1, 2, 3, 4, 6

curve was fitted to the entire data-set. We estimated the ultimate fraction of particles passing the selected location as the asymptote of the fitted curve.

In some cases the curve could not be fit to the data, or the fit was poor; generally, this occurred under low-flow conditions when particles began arriving at distant points late in the simulation and were continuing to accumulate at the end of the simulation rather than approaching an asymptote. In those cases, the 90-day value was used as an estimate of the ultimate value.

In addition to the ultimate fate of particles, we calculated a measure of residence time. The value chosen was the time for 75% of the particles to leave the Delta. We selected this value because we were most concerned about how long it takes a group of particles (representing plankton) to leave the Delta, but we also wanted a statistically robust metric. In a handful

of cases, 75% of the particles had not left the Delta by the end of the model run, and this time had to be determined on the extrapolated curve as described above. In one case it was determined by eye.

The ultimate fraction of particles lost to the export facilities and, in some model runs, to agricultural diversions, was modeled as a function of the export:inflow (EI) ratio. The EI ratio is used in management of the Delta because it is assumed to provide a measure of the influence of south Delta diversions (Newman and Rice 2002). By regulation, the EI ratio must not exceed 35% during February–June or 65% for the rest of the year. The model was a logistic curve fit to the data by using an optimizing program to minimize the sum of squared differences between the data and the curve. The curve was fit separately for each release site. In contrast to particle fate, the relationship of residence time to inflow and export

flow was examined graphically, since no underlying model seemed to apply to all release sites.

All analyses were conducted in S-PLUS (Venables and Ripley 2003). Analyses were checked at several steps to eliminate programming errors. Checks included random or systematic comparisons of unfiltered and filtered output, graphical examination of cumulative particle passage with model outputs superimposed, and other such cross-checks. Model output is available from the authors upon request.

### Case Studies

We conducted two case studies that may be helpful in thinking about managing the Delta to protect fish populations. Larvae and early juveniles of delta smelt occur in the Delta in spring when they are vulnerable to entrainment in the south Delta export facilities (Moyle et al. 1992, Bennett 2005). We used data from the California Department of Fish and Game 20-mm survey of late larval and juvenile fish (Dege and Brown 2004), selecting surveys from three years (2001–2003) of low outflow, and averaging catch per trawl of <10mm larvae for each station over all surveys. The assumption was that in these dry years the population would be slow to move out of the Delta, so the abundance of small fish could be used to approximate the spatial distribution of hatching. Each PTM release site was linked with the nearest sampling station, and the mean catch per trawl was used to provide a weighting factor for the release site. The proportion of particles that moved within 30 days from each site to the export facilities, and the mean loss weighted by delta smelt abundance, were determined for each set of flow conditions and examined graphically.

Juvenile Sacramento River Chinook salmon may be exposed to the export pumps if they stray from the Sacramento River during migration to the sea. Mark-recapture experiments have been conducted in winter in the northern Delta to examine the effect of pumping on endangered winter Chinook (Brandes and McLain 2001; Newman 2003). Fish marked with coded-wire tags are released at Ryde on the mainstem Sacramento River and in Georgiana Slough, from which they move with the net flow into the interior

Delta (See Figure 1). Fish are recaptured either in a trawl survey at Chipps Island or in the ocean fishery. The ratio of apparent survival of the two groups of fish is used as a measure of the relative survival by the two pathways, and is then related to export flow. Results of these and similar experiments conducted in the spring have been inconclusive regarding the influence of export flow and DCC gate position on subsequent survival (Newman and Rice 2002; Newman 2003). We used the ratio of particles passing Chipps Island from releases in Georgiana Slough and at Ryde as a parallel measure of “survival,” and related that to inflow and export flow.

### RESULTS

Replicate particle releases with different random number seeds resulted in minor variability in the ultimate fate of particles (Table 5). Standard deviations of the percentage of particles arriving at export facilities or Chipps Island were generally ~ 0.5% or less. This introduces some error into our calculations, which has a minor effect on the parameters of our models.

Raw data, expressed as the cumulative percentage of particles passing a point, show tidal effects that vary with location, and to some degree, between spring and neap tide (Figure 3). For releases along the Sacramento River and western Delta with low inflow ( $340 \text{ m}^3 \text{ s}^{-1}$ ) and export flow ( $57 \text{ m}^3 \text{ s}^{-1}$ ), tidal effects were strong for particle flux past Chipps Island because large tidal excursions coincided with strong spatial gradients in concentration (Figure 3A).

**Table 5.** Ultimate fate of particles from replicate releases at the Hood site.

Final Location	Inflow	Export	Mean Particles	% of Standard Deviation
Chipps Island	340	57	83.4	0.44
Chipps Island	340	283	15.6	0.57
CVP	340	283	26.9	0.31
SWP	340	283	49.8	0.45
Chipps Island	1,077	170	94.1	0.15
Chipps Island	3,401	170	98.5	0.13

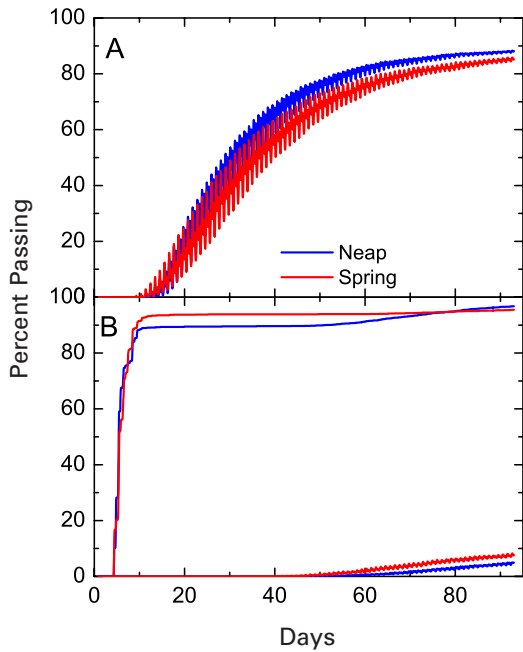


**Figure 3.** Cumulative passage at Chipps Island and export facilities during during low inflow and export flow and spring and neap tides for: A) Releases at Hood and recoveries at Chipps Island, and B) Releases at Vernalis and recoveries at export facilities (top) and Chipps Island (bottom).

Effects in the southern Delta were much less pronounced because of smaller tidal excursions and a longer transit time, which reduced spatial gradients (Figure 3B). Differences between spring and neap tides were most apparent in tidal variability and less so in timing of movement and ultimate fate. The principal effect of spring tides was to spread the particles out, increasing the variety of pathways that they took.

Particle fates on spring and neap tides did not differ markedly (Figure 4). The general trends were for lower losses to export pumping and longer times to leave the Delta on spring tides than on neap tides. The difference in losses was most pronounced in the eastern Delta (~ 10% in some cases), although releases from the southern Delta had high proportional increases in the fraction of particles that left the Delta via Chipps Island. For example, about 9% of the particles released at Vernalis on a spring tide eventually passed Chipps Island, whereas fewer than 1% of the particles did so on a neap tide. The tidal

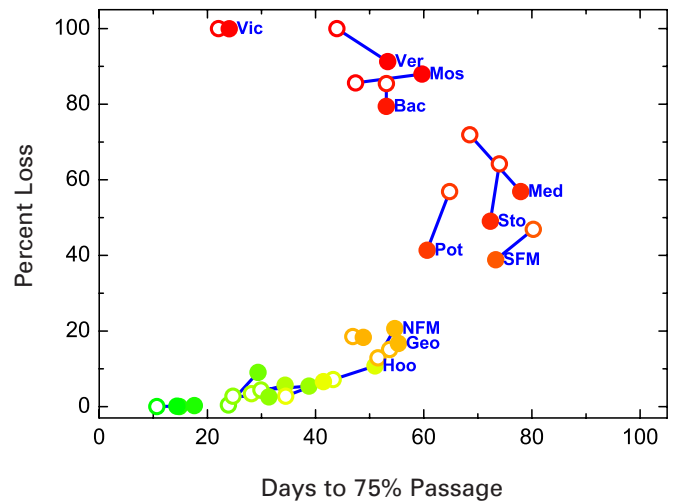


**Figure 4.** Effect of spring vs. neap tides on time for 75% of particles to leave the Delta vs. the proportion of particles lost to export facilities for low inflow ( $340 \text{ m}^3 \text{ s}^{-1}$ ) and export flow ( $57 \text{ m}^3 \text{ s}^{-1}$ ). Open symbols, neap tide; filled symbols, spring tide; lines connect spring and neap points. Symbol colors represent initial locations as in Figure 1. Labels on some points give release location (see Table 4); others are omitted for clarity.

influence on residence time was strongest along the Sacramento and San Joaquin Rivers, and occurred because more particles were mixed into alternative pathways from which they took longer to exit the system. All of these differences were much smaller at higher flow and export levels (not shown).

Subsequent results are for spring tides only, since tide had relatively small effects on the ultimate fate of particles, but could extend residence time in the Delta under some conditions. The influence of net flows in the Delta is illustrated by example model runs from releases at Hood under four contrasting flow conditions (Figure 5). With low inflow and export flow, only about 85% of the particles had left the Delta by the end of the 90-day run (Figure 5A). The passage of particles was delayed by movement of particles into the central Delta, which increased travel time. In contrast, low inflow and high export flow caused most particles to go to the export facilities (Figure 5B). With high inflow, the fate of the particles was determined rapidly, and a smaller fraction entered the central Delta (Figure 5C). Even with high export flow, relatively few particles ended up at the south Delta export facilities if inflow was high (Figure 5D).

The fate of particles was reversed for releases in the San Joaquin River at Mossdale (Figure 6). There, most of the particles ended up at the export facilities, particularly the CVP, except that high inflows moved a substantial fraction to Chipps Island, and a larger fraction were entrained into the SWP (via the lower San Joaquin River) than was the case with low inflows.

Combining the results of all model runs under spring tides with no agricultural diversions, no agricultural barriers, and the DCC open at flows below  $600 \text{ m}^3 \text{ s}^{-1}$ , we see the predicted effect of flows on the ultimate fraction of particles exported (Figure 7). For each release site, the fraction lost to export flow could be modeled as a logistic function of the export:inflow (EI) ratio. The parameters of the logistic function differed for each site, so that very high EI ratios were necessary to move large fractions of particles from the north Delta to the pumps, whereas only at the lowest EI ratios would substantial fractions of particles from the southern Delta escape entrainment. Variations in fit of the data to the model under high and low flows with similar EI ratios can be seen, for example, in the parallel rows of points for releases at Franks Tract East (Figure 7). These variations suggest that the EI model is not perfect, but no alternative model was found that provided a superior fit to the data.

The above model is over-simplified in that the ultimate fate of the particles can be interpreted only in the context of the time it takes to reach that fate. The day on which 75% of the particles had left the Delta (Figure 8) generally decreased with increasing inflow, reflecting the decrease in hydraulic replacement time with increasing flow (gray lines in Figure 8). In the northern Delta, the 75% time was close to the hydraulic replacement time, whereas in the central and southern Delta it was often much longer. Effects of export flow also varied substantially among release locations. For release sites in the northern Delta, increasing export flow increased net flow and decreased residence time at low inflow. In the central Delta, this effect was reversed at low inflow, because increasing export flow decreased net flow; at higher inflows the effect of export flow in the central Delta was additive as in the northern

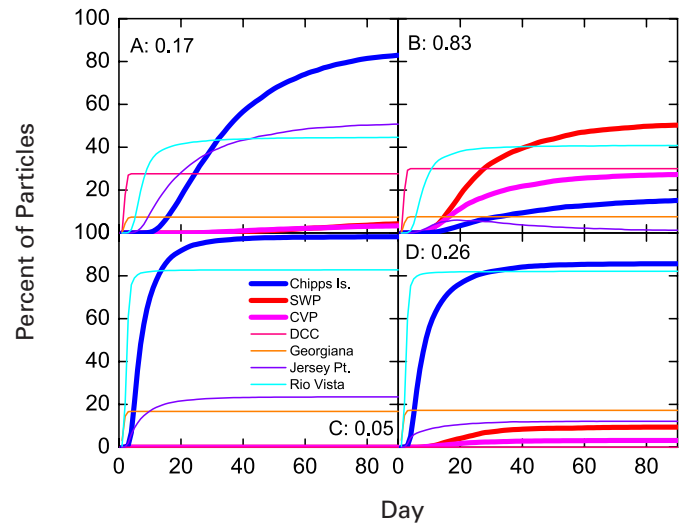


**Figure 5.** Time course of tidally-averaged particle passage for releases from Hood during spring tides for four flow conditions. Thin lines denote intermediate locations, and thick lines denote final locations by which particles leave the model domain (Figure 1). Numbers give export:inflow ratios. A and B have inflow at  $340 \text{ m}^3 \text{ s}^{-1}$ , C and D have inflow at  $1,078 \text{ m}^3 \text{ s}^{-1}$ . A and C have export flow at  $57 \text{ m}^3 \text{ s}^{-1}$ , and B and D have export flow at  $283 \text{ m}^3 \text{ s}^{-1}$ .

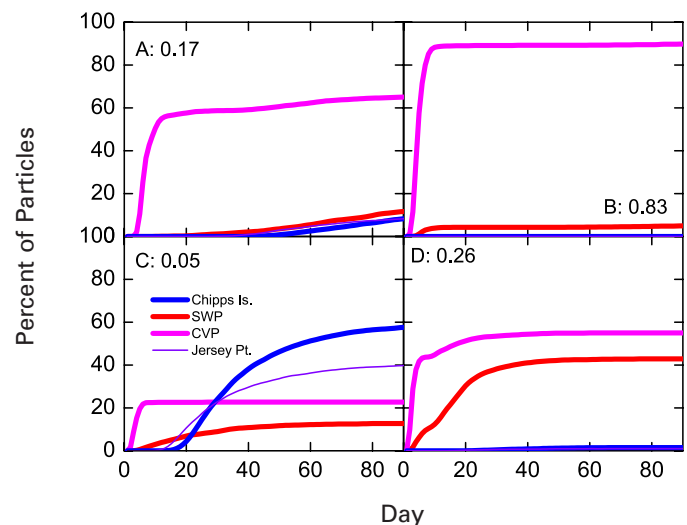


**Figure 6.** As in Figure 5, for releases at Mossdale, intermediate locations include only Jersey Point because few or no particles from Mossdale reached the other intermediate locations.

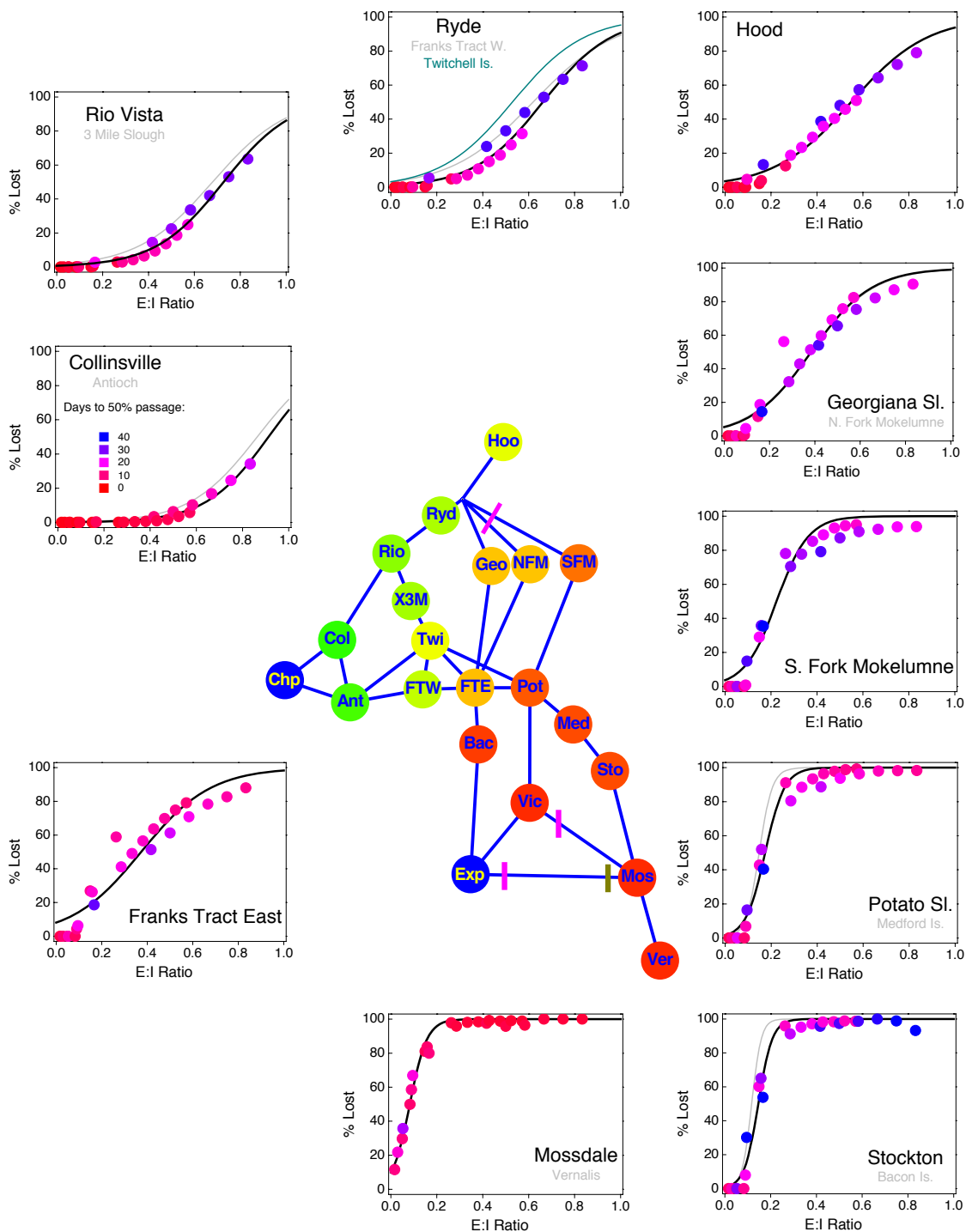


**Figure 7.** Percent of particles lost to export pumps for spring tide runs with no agricultural diversions and 24 combinations of inflow and export flow. Data are shown for selected release sites, color-coded by the time needed for 75% of particles to leave the Delta. Lines are logistic functions fit to the data, and are dark for selected sites and light gray for other sites with similar responses. Central diagram is a schematic arrangement of the sites in Figure 1, with principal links between sites. Short lines represent barriers including the DCC in the northern Delta, the Head of Old River barrier in the south Delta (dark yellow), and south Delta agricultural barriers (pink).

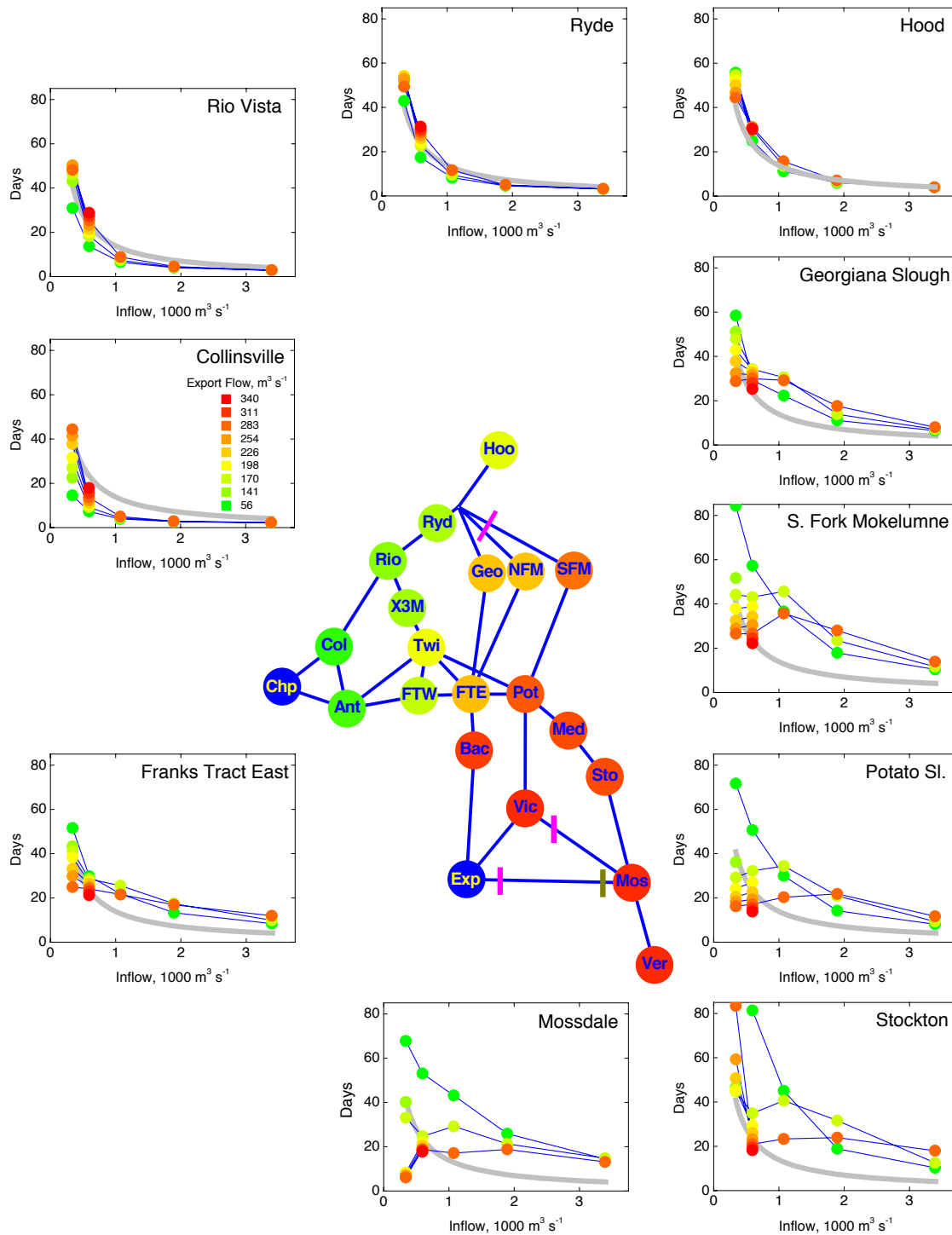


**Figure 8.** Relationship between the time for 75% of particles to exit the Delta and inflow and export flow. Diagrammed as in Figure 7. Colors on graphs scale export flow from the lowest (green) to the highest (red). Heavy gray lines give the hydraulic residence time, calculated as the volume of the Delta ( $1.2 \times 10^9 \text{ m}^3$ ) divided by total Delta inflow.



Delta (e.g., the South Fork of the Mokelumne River, Figure 8). The response of residence time to inflow in the southern Delta was mixed: at low export flow, the response was similar to but much longer than hydraulic replacement time, whereas at high export flow, the effect of inflow was muted or even reversed (e.g., Mossdale, Figure 8).

Residence time for releases at Mossdale and Stockton differed in some revealing ways despite the proximity (29 river km) of these two stations. Particles released at Mossdale can enter upper Old and Middle Rivers and go west directly to the export facilities, whereas particles released at Stockton get to the export facilities only by way of the San Joaquin River and southerly net flow in lower Old and Middle Rivers. This means that low inflow and low to moderate export flow can result in long residence times; for example, at the lowest combination of inflow and export flow, the time for 75% of the particles to leave the Delta from Stockton exceeded 90 days (Figure 8).

The effect of agricultural diversions on the fate of particles is rather predictable: higher agricultural diversions increase the proportion of particles lost to total diversions. This has the effect of shifting the logistic curves in Figure 7 to a lower EI ratio (Figure 9) and somewhat decreases the residence time. Combining all results, the EI ratio resulting in a given percent loss decreases predictably across all release sites (Figure 10). The effect of agricultural diversions on the time for 75% of the particles to leave the Delta depends on release site: this time increases for sites in the northern Delta and decreases for sites in the central or southern Delta (Figure 11). This is because the ultimate fates differ: particles released in the northern Delta go mainly to Chipps Island, and are retarded from going there when agricultural diversions reduce outflow. Particles released in the central and southern Delta tend to have high residence times at low flows, but residence times are reduced by losses to agricultural diversions.

The effect of the Delta Cross Channel on the ultimate fate and timing of particles released in the northern Delta was unexpected (Figure 12). For releases at Georgiana Slough and Ryde, closing the DCC increased the percentage of particles entrained in the

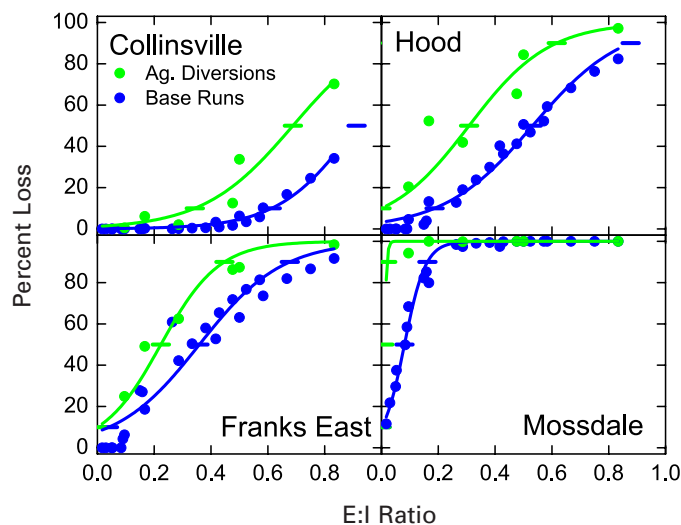


**Figure 9.** Examples of the effects of agricultural diversions. For these four release sites, the relationship of percent of particles lost to the pumps and agricultural diversions is plotted against export:inflow ratio for base runs (shown in Figure 7) and runs with agricultural diversions set to their summer maximum. Short horizontal lines give the quantiles at which export:inflow ratios were calculated for Figure 10.

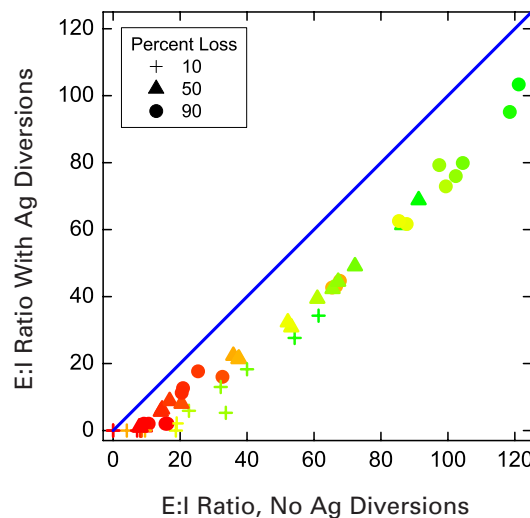


**Figure 10.** Summary of effects of agricultural diversions for all release sites, showing the required export:inflow ratios for 10, 50, and 90% combined losses to export pumping in the south Delta and agricultural diversions. Each point is derived from logistic curves as in Figure 9. Colors correspond to stations in the diagram in Figure 1.

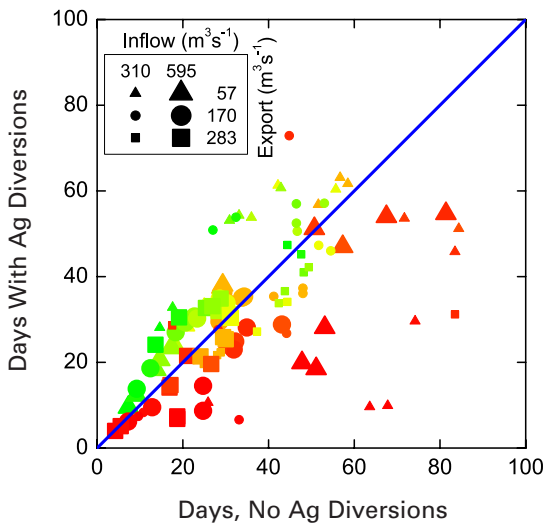


**Figure 11.** Effect of agricultural diversions on the time at which 75% of particles have left the Delta. Symbol colors represent initial locations as in Figure 1. Symbol sizes give inflow in two categories, and shapes give export flow in three categories.

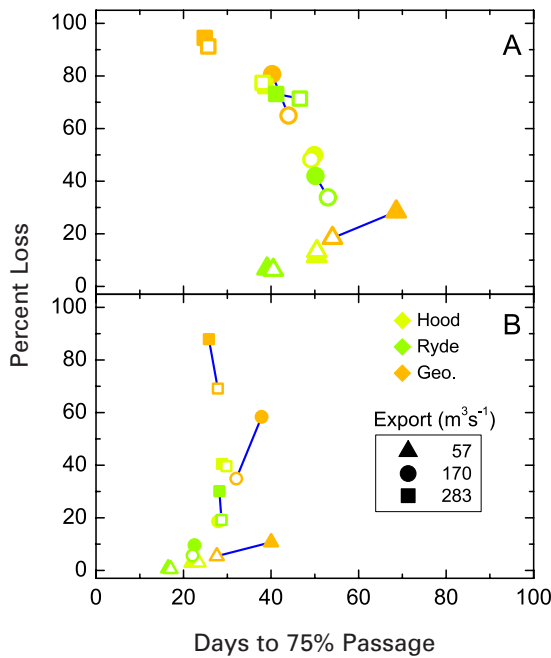


**Figure 12.** Effect of DCC on time for 75% of particles to leave the Delta vs. proportion of particles lost to the export facilities. A) Inflow of  $340 \text{ m}^3 \text{ s}^{-1}$ ; B) Inflow of  $595 \text{ m}^3 \text{ s}^{-1}$ . Open symbols mean DCC open; filled symbols mean DCC closed. The effect of opening the DCC is shown by a line connecting a closed symbol to an open symbol for each set of conditions. Symbol colors represent initial locations as in Figure 1, and shapes give export flow in three categories.

pumping plants and decreased the percentage that passed Chippis Island. For Georgiana Slough, closing the DCC at low export flow rates also increased the residence time of particles. Effects on particle fate were more pronounced at higher flows, while effects on residence time were more pronounced at lower flows.

Closing the DCC alters the pathways of particles from the Sacramento River to the central Delta, but has relatively little effect on overall entrainment except for the release site in Georgiana Slough (Figure 13). Releases at Sacramento and at Hood (Figure 13A, B) had very similar responses. With the DCC closed, about the same proportion of particles was lost to pumping as when it was open; to make up for the loss of the DCC pathway, a greater proportion of particles arrived at the export facilities through Georgiana Slough, Three-Mile Slough at moderate to high export rates, and the lower San Joaquin River at high export rates.

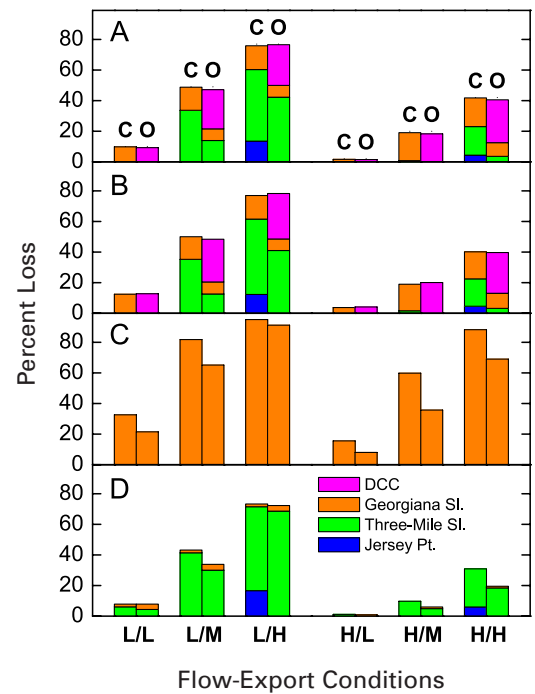


**Figure 13.** Delta Cross Channel effects. Contributions of various pathways to percentage of particles lost to combined CVP and SWP pumping. Each bar gives the contribution of each of four pathways. Release sites were: A) Sacramento; B) Hood; C) Georgiana Slough; D) Ryde (see Figure 1). Flow and export conditions are given in Table 2. C and O in panel A means position of the DCC gates (closed or open) and applies to all panels.

The temporary barriers in the southern Delta had modest effects on the ultimate fate and residence time of particles (Figures 14–15). Adding the three agricultural barriers (Figure 7) reduced losses from the southern and central Delta at low export rates, and either increased (southern Delta) or decreased (central to northern Delta) the residence time of particles (Figure 14). At higher export rates, the only effect of the barriers was to increase residence time of particles released in the southern Delta. The barrier at the head of Old River (Figure 1) reduced losses by ~20% and increased particle residence time at the lowest export rates; at higher export rates, nearly all of the particles were lost to export pumping, irrespective of barrier position.

The simulation of delta smelt losses showed substantial cumulative losses could occur under some flow conditions (Figure 16). Losses increased with increasing export flow and with decreasing inflow. The simulation of mark-recapture experiments of Chinook salmon in the northern Delta showed similar results (Figure 17). The ratio of particles passing Chipps Island from releases in Georgiana Slough to those from Ryde increased with inflow, and decreased strongly with increasing export flow, particularly when inflow was low to moderate. The effect of opening the DCC was to increase the predicted recovery ratio (Georgiana Slough:Ryde).

## DISCUSSION

The fundamental assumptions of a particle tracking model (PTM) are that the hydrodynamic representation is reasonably accurate, and the behavior of the particles represents some behavior of interest. DSM2 represents flow and salinity quite accurately (Appendix), reflecting the great effort that has gone into refining the bathymetric data and into calibrating the model to Delta conditions. This has come about mainly because DSM2 is being used as a tool for managing water and for keeping salinity below limits, though it is unfortunate that none of the calibration information has been published and subjected to peer review given this reliance on the model. Thus, we have a reasonable degree of confidence that the basic hydrodynamic and water quality modules pro-

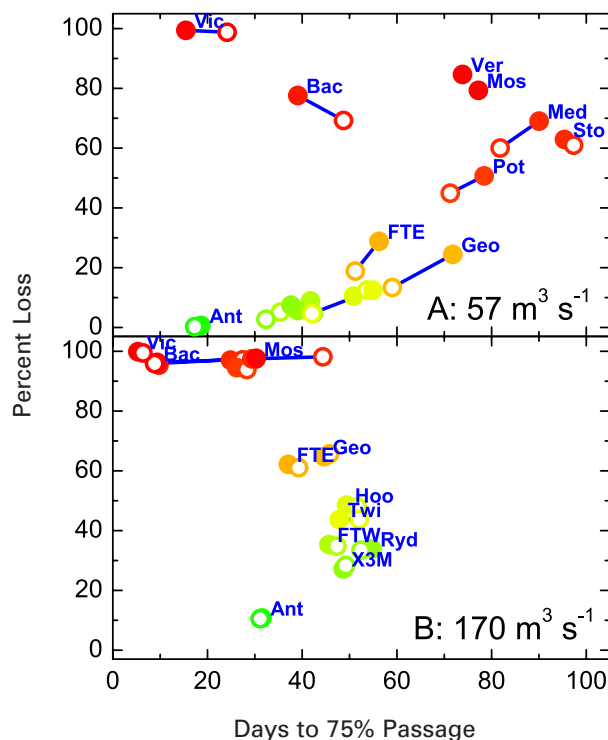


**Figure 14.** Effect of south Delta agricultural barriers on time for 75% of particles to leave the Delta vs. proportion of particles lost to export facilities. Open symbols, barriers absent; filled symbols, barriers in place. Symbol colors represent initial locations as in Figure 1.

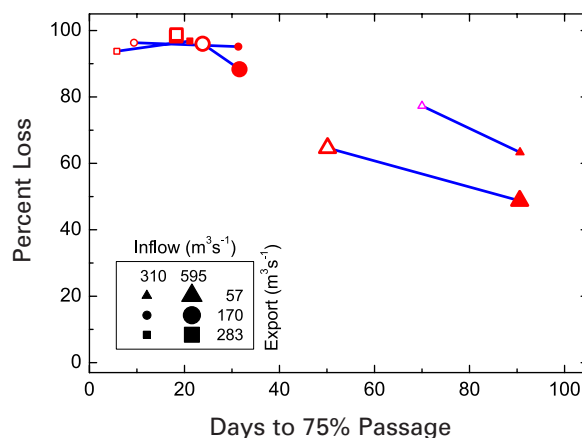


**Figure 15.** As in Figure 14 for the barrier at the Head of Old River, releases at Mossdale only; releases at Vernalis have nearly identical patterns.

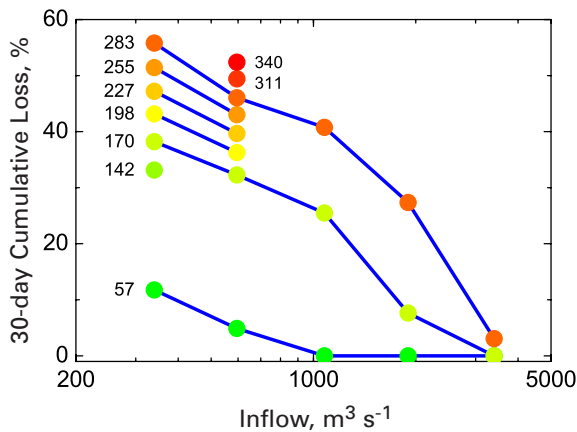


**Figure 16.** Effect of changing inflow and export flow on modeled fractional losses of delta smelt larvae over a 30-day period. Lines connect data with the same export flow indicated by color. Numbers give export flows.

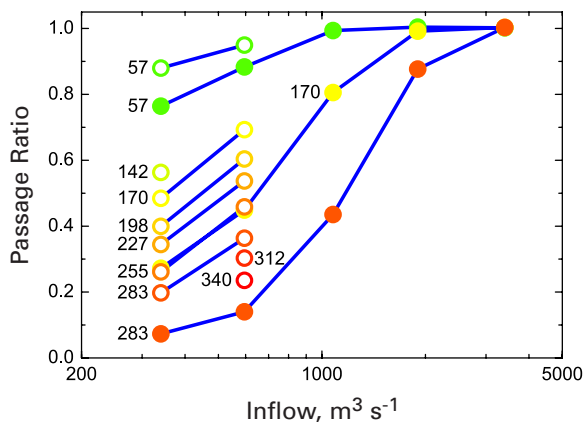


**Figure 17.** Effect of export flow, inflow, and DCC gate position on the ratio of proportion of particles passing Chipps Island from releases in Georgiana Slough to that for releases at Ryde. Symbols are the same as in Figure 16 except: open symbols mean DCC open; filled symbols mean DCC closed. Numbers give export flows.

vide usable output. However, the PTM has not been calibrated, and it differs enough from the water quality module to suggest caution in interpreting our results. In particular, tidal effects would be most strongly influenced by the method used to track particles through junctions, namely through complete mixing at each junction. This method is less likely to influence advective transport than dispersion, and the results of these model runs suggest advection-dominance most of the time (Figure 4).

The use of PTMs for investigating ecological issues has been increasing (e.g., Garvine et al. 1997; Brown et al. 2005; North et al. 2005). This reflects better hydrodynamic modeling, improved resolution of organism behavior, and greater interest in how organism movement interacts with flow fields. Another stimulus for interest in PTMs is that conceptually they are related to individual-based models (IBMs), and can be considered a simplified case of IBMs. Indeed, IBMs are often embedded as PTMs in models of ocean circulation or mixing (e.g., Batchelder et al. 2002; Hofmann et al. 2004).

Our use of a PTM focuses on life stages of fish with limited mobility, particularly delta smelt larvae, and our region of interest is the entire Delta. We chose not to give particles behavior in these model runs because we had little basis for determining what that behavior should be. Thus, the results presented here may be less applicable to larger, more competent organisms (but see Implications for Chinook Salmon, below).

One striking result of our modeling is that selecting a particular time period, such as the larval period of a fish, gives results that might be easy to interpret for that particular purpose but which will also be difficult to relate quantitatively with environmental conditions. For example, low export flows result in relatively low entrainment from all stations, but they also cause very slow transport through the southern Delta. Thus, a short time horizon might give an optimistically low proportion of particles entrained in the south Delta pumping plants, simply because the particles are still mostly at large in the Delta at the end of the model run. This is why we focused on the ultimate fate of the particles, and used residence time (as

scaled by the time for 75% of the particles to leave the Delta) as an additional measure.

A consequence of this is that simple questions (e.g., what proportion of particles are entrained under a given set of conditions) have no clear answer. Instead, the answer depends on the time horizon, which in turn depends on the overall flow conditions and the site of the release. We are, furthermore, not inclined to define a “zone of influence” of the pumps on the basis of our results, since the probability of entrainment depends on time horizon which, in many cases, is too long to be useful for analyzing the movements of larval fish. By the end of the modeled time period, the fish would already have metamorphosed, and their behavior would have become more complex.

The export:inflow (EI) ratio proved useful as a predictor of the ultimate fate of particles, subject to several caveats. We were surprised at how well the logistic models of EI ratio fit the data on proportional entrainment (Figure 7), because our working hypothesis was that the EI ratio was too simplistic, and too much based on net, non-tidal flow, to be useful. The EI ratio was useful as a predictor of probability of entrainment, provided the model was allowed to run long enough to resolve the particles' ultimate fate. Over shorter time periods, the EI ratio is less predictive because of the dependence of residence time on overall flow conditions (Figure 8). Furthermore, the relationship of percent loss to EI ratio was logistic, which makes sense given the mechanisms but also requires a nonlinear fit to the data.

The relationship of particle residence time to flow conditions was expected. Hydraulic replacement time (i.e., volume of the Delta divided by inflow) is roughly proportional to the inverse of inflow (Figure 8), and this is reflected in the time for 75% of particles to leave the Sacramento River (where export effects are small). At low inflows, dispersion and export flows have a greater relative impact, so the residence time is shorter than the hydraulic replacement time. In the southern Delta, by contrast, particle residence times were generally much longer, and strongly influenced by export flows. This illustrates a contrast

between the river-dominated northern Delta and the southern Delta where advection is weak and driven largely by export pumping. However, in both regions, net particle movements were largely determined by advection, with tides serving mainly to spread out and delay the passage of particles by the observation points (Figures 3–4).

Agricultural diversions have the effect of lowering the EI ratio needed for a given percentage loss to diversions, i.e., shifting the curves in Figure 7 to the left as in Figure 9. This effect is strongest in the south Delta because entrainment probability is so high under most flow conditions. The effect of agricultural diversions on residence time depends on the initial release site, and varies with inflow and export flow, but would be difficult to predict in general.

### Implications for Chinook Salmon

Salmon smolts are not particles; they have complex behaviors and are strong swimmers. We do not know what cues them to navigate downstream and out to the ocean. However, there are two reasons why PTM results may be informative with regard to salmon. First, whether the fish have strongly directed movement or not, they swim in the channels where they are subject to tidal and residual currents, and thus they will be distributed among alternative pathways during downstream migration, since it seems unlikely that they can distinguish among pathways. Although this distribution may differ from that of the water, it will still result in a dispersive movement pattern. Second, a recent unpublished report on radio tracking of larger yearling Chinook salmon concluded that the movement of the fish could not be distinguished from tidal excursions, and that any seaward-directed movement must be subtle (Vogel 2004). We do not claim that the specific results presented here represent actual movements of salmon; rather, these results indicate what factors may or may not be important in determining how salmon smolts may move through the Delta.

The DCC had smaller effects than anticipated, with virtually no effect on the ultimate fate of particles released upstream of it, and a small effect on residence time. Apparently, closing the DCC gates sim-



ply raises head in the Sacramento River, causing more water and particles to enter the central Delta via other pathways (Figure 13). This contrasts with results of paired mark-recapture experiments with hatchery-reared salmon, which gave a significant effect of gate position in two of three alternative statistical analyses (Newman 2003).

Releases downstream, particularly those in Georgiana Slough, had a greater probability of entrainment in the export pumps when the DCC was closed than when it was open, because of the greater southward net flow in Georgiana Slough and presumably also Three-Mile Slough. Releases at Sacramento and Hood had almost identical fates, indicating that few particles were diverted into Steamboat and Sutter Sloughs to the north of the mainstem Sacramento River, where they would escape entrainment into the central Delta.

Model runs to examine the proportion of particles that arrive at Chipps Island of those released in Georgiana Slough vs. in the mainstem Sacramento River at Ryde showed that both inflow (related to Sacramento River flow) and export flow had important influences. At the highest inflows, the ratio of particle passage was close to 1 (Figure 17). At lower inflows, fewer of the particles released in Georgiana Slough arrived at Chipps Island compared to the Ryde releases, and this effect was stronger at higher export flows. Data from mark-recapture experiments (Brandes and McLain 2001; Newman 2003) gave rather different results for tagged hatchery-reared salmon: most of the survival ratios were low, even when river flow was high (median 0.26 for inflow  $> 1,000 \text{ m}^3 \text{ s}^{-1}$ ; data from P.L. Brandes, U.S. Fish and Wildlife Service, pers. comm.), and survival ratios were only weakly related to export flow and apparently not to inflow or river flow. There are several potential reasons for this difference. It may merely reflect the difference in behavior between salmon smolts and neutrally-buoyant particles. The fish appear to survive poorly in Georgiana Slough, irrespective of flow, possibly because of differences in habitat conditions between the mainstem Sacramento River and the interior Delta (Nobriga et al. 2005). In addition, the recapture rate for the Chipps Island trawl is low and therefore highly variable, and recap-

tures of the fish released in Georgiana Slough may be biased low because the longer migration period results in lower daily recapture rate. Despite all these differences, the PTM results suggest that river flow may be an important variable in determining which way the salmon go and their probability of survival, and should be included in the design and analysis of future studies.

The movable barriers in the southern Delta had a relatively small effect on losses from releases at Mossdale and Vernalis, and a moderate effect on particle residence time. Losses were reduced with the barriers in place, but only at moderate inflow. The barrier at the head of Old River is there to protect salmon from entrainment, but it has little effect on particle fate under flow conditions that result in high entrainment without the barrier.

The Vernalis Adaptive Management Program (VAMP, SJRGA 2006) is intended to reduce entrainment of Chinook smolts migrating down the lower San Joaquin River, and to investigate the influence of alternative river flows and export flows on the survival of marked salmon. The EI ratio typical of the VAMP experimental period is around 10% (as defined here), so entrainment losses should be low (Figures 6C, 7). However, at low flow in the San Joaquin River and low export flow, the time for passage can be very long, with the likely result of higher mortality and lower detection, at least in the Chipps Island trawl survey. Results of the VAMP studies have often shown very low survival for fish released at Mossdale or just below the junctions with Old and Middle Rivers, and relationships of survival to flow conditions appear weak. We believe this is partly because of the small range of inflow and export flow being tested.

### Implications for Delta Smelt

Previous analyses have suggested that delta smelt larvae may be highly vulnerable to export losses (Bennett 2005). Furthermore, the delta smelt population is further seaward and away from the export facilities when freshwater outflow (roughly equal to inflow minus export flow) is high and the salt field is seaward (Dege and Brown 2004). Our PTM results



suggest a direct link between the position of the smelt population as determined by outflow, and losses as determined by export flow (Figure 16). Results of analyses of larval delta smelt losses are rather similar to those from our PTM studies (Kimmerer 2008). These findings may be enough to recommend strong protective measures for delta smelt in spring (March–May) of low outflow years when they are highly vulnerable to export losses.

We are less confident about estimating entrainment effects on other life stages, since delta smelt appear able to maintain their position in the estuary, generally in brackish water, beginning at the late larval stage. During their spawning migration they are again vulnerable to export effects, but because adult movements may be directed, the PTM is less suitable for analyzing the probability of entrainment of these fish without an improved understanding of adult migratory behavior.

## CONCLUSIONS

This project demonstrates the capabilities and some of the uses of the PTM. The key lesson seems to be the importance of residence time in measuring and interpreting the fate of particles.

Limitations of the model should also be borne in mind. Since DSM2 is calibrated to the existing Delta, it is not a particularly suitable tool for examining alternative physical configurations such as levee failures. It does not represent stratification, does not conserve momentum at channel junctions, and may not represent open-water areas of the Delta very well. However, for examining Delta-wide movements of particles meant to represent fish, these drawbacks appear fairly minor compared with the problem of defining the behavior of the fish. To the extent that fish allow themselves to be dispersed by tidal and river currents, this model is likely suitable for describing Delta-wide movement. This conclusion is contingent upon comparisons of the model with QUAL or, better, 2-D or 3-D model runs, to provide a firmer basis for using DSM2.

Numerous opportunities remain for studies using this model. We examined a limited suite of environmen-

tal conditions, and, in particular, we did not vary the proportions of flow between the Sacramento and San Joaquin Rivers, or between the export facilities. Future studies could also make use of the PTM's capability for assigning behaviors to particles, although 3-D models now becoming available will be much more useful and reliable for that purpose.

## ACKNOWLEDGEMENTS

This study was funded by the Interagency Ecological Program for the San Francisco Estuary (IEP). We greatly appreciate the help of A. Miller (California Department of Water Resources) who assisted the authors with model set-up and who developed the hydrologic files for this project. We also thank B. Suits, T. Smith, and C. Enright (CDWR) and W. Bennett (UC Davis) for their insight during initial project development. Thanks to P. Brandes for data on salmon survival. We appreciate helpful comments on an earlier draft by S. Culberson and A. Miller. Finally, we thank S. Monismith and E. Gross for extensive comments and discussions on the manuscript.

## REFERENCES

- Batchelder HP, Edwards CA, Powell TM. 2002. Individual-based models of copepod populations in coastal upwelling regions: implications of physiologically and environmentally influenced diel vertical migration on demographic success and nearshore retention. *Progress in Oceanography* 53(2-4):307–333.
- Bennett WA. 2005. Critical assessment of the delta smelt population in the San Francisco Estuary, California. *San Francisco Estuary and Watershed Science* [Internet]. 3(2). Available from: <http://repositories.cdlib.org/jmie/sfews/vol3/iss2/art1>
- Brandes PL, McLain JS. 2001. Juvenile Chinook salmon abundance, distribution, and survival in the Sacramento-San Joaquin Estuary. In: Brown RL, editor. *Contributions to the biology of Central Valley salmonids*. California Department of Fish and Game Fish Bulletin 179. p 39–137. Available from: <http://repositories.cdlib.org/sio/lib/fb/179/>

- Brown CA, Jackson GA, Holt SA, Holt GJ. 2005. Spatial and temporal patterns in modeled particle transport to estuarine habitat with comparisons to larval fish settlement patterns. *Estuarine, Coastal and Shelf Science* 64(1):33–46.
- Brown RL. 1982. Screening agricultural diversions in the Sacramento-San Joaquin Delta. California Department of Water Resources Report.
- Brown R, Greene S, Coulston P, Barrow S. 1996. An evaluation of the effectiveness of fish salvage operations at the intake of the California Aqueduct, 1979–1993. In: Hollibaugh JT, editor. *San Francisco Bay: the ecosystem*. San Francisco (CA): Pacific Division of the American Association for the Advancement of Science. p 497–518.
- CDWR (California Department of Water Resources). 2001. Methodology for flow and salinity estimates in the Sacramento-San Joaquin Delta and Suisun Marsh. Twenty-second annual progress report to the State Water Resources Control Board. Available from: <http://modeling.water.ca.gov/Delta/reports>.
- Cronin TW, Forward Jr. RB. 1979. Tidal vertical migration: an endogenous rhythm in estuarine crab larvae. *Science* 205(7 Sep/4410):1020–1022.
- Culberson SD, Harrison CB, Enright C, Nobriga ML. 2004. Sensitivity of larval fish transport to location, timing, and behavior using a particle tracking model in Suisun Marsh, California. In: Feyrer F, Brown LR, Brown RL, Orsi JJ, editors. *Early life history of fishes in the San Francisco Estuary and watershed*. Bethesda (MD): American Fisheries Society. p 257–267.
- Dege M, Brown LR. 2004. Effect of outflow on spring and summertime distribution and abundance of larval and juvenile fishes in the upper San Francisco Estuary. In: Feyrer F, Brown RL, Brown LR, editors. *Early life history of fishes in the San Francisco Estuary and watershed*. American Fisheries Society Symposium 39. p 49–65.
- Dew CB, Hecht JH. 1994. Hatching, estuarine transport, and distribution of larval and early juvenile Atlantic tomcod, *Microgadus tomcod*, in the Hudson River. *Estuaries* 17(2):472–488.
- Garvine RW, Epifanio CE, Epifanio CC, Wong K-C. 1997. Transport and recruitment of blue crab larvae: a model with advection and mortality. *Estuarine, Coastal, and Shelf Science* 45:99–111.
- Herren JR, Kawasaki SS. 2001. Inventory of water diversions in four geographic areas in California's Central Valley. In: Brown RL, editor. *Contributions to the biology of Central Valley salmonids*. California Department of Fish and Game Fish Bulletin 179. p 343–355. Available from: <http://repositories.cdlib.org/sio/lib/fb/179/>
- Hofmann EE, Haskell AGE, Klinck JM, Lascara CM. 2004. Lagrangian modelling studies of Antarctic krill (*Euphausia superba*) swarm formation. *ICES Journal of Marine Science* 61:617–631.
- Jassby AD, Kimmerer WJ, Monismith SG, Armor C, Cloern JE, Powell TM, Schubel JR, Vendliniski TJ. 1995. Isohaline position as a habitat indicator for estuarine populations. *Ecological Applications* 5(1):272–289.
- Kimmerer WJ. 2002. Physical, biological, and management responses to variable freshwater flow into the San Francisco Estuary. *Estuaries* 25(6B):1275–1290.
- Kimmerer WJ. 2008. Losses of winter-run Chinook salmon and delta smelt to export entrainment in the southern Sacramento-San Joaquin Delta. *San Francisco Estuary and Watershed Science*. [Internet]. 6(1). Available from: <http://repositories.cdlib.org/jmie/sfews/> (in press).
- Kimmerer WJ, Burau JR, Bennett WA. 2002. Persistence of tidally-oriented vertical migration by zooplankton in a temperate estuary. *Estuaries* 25(3):359–371.
- Kimmerer WJ, Cowan Jr. JH, Miller LW, Rose KA. 2001. Analysis of an estuarine striped bass population: effects of environmental conditions during early life. *Estuaries* 24(4):557–574.
- Livingston RJ, Niu X, Lewis III FG, Woodsum GC. 1997. Freshwater input to a gulf estuary: long-term control of trophic organization. *Ecological Applications* 7(1):277–299.

## SAN FRANCISCO ESTUARY & WATERSHED SCIENCE

- Moyle PB. 2002. Inland fishes of California: revised and expanded. Berkeley (CA): University of California Press.
- Moyle PB, Herbold B, Stevens DE, Miller LW. 1992. Life history and status of delta smelt in the Sacramento-San Joaquin Estuary, California. *Transactions of the American Fisheries Society* 121(1):67-77.
- Moyle PB, Israel JA. 2005. Untested assumptions: effectiveness of screening diversions for conservation of fish populations. *Fisheries* 30(5/May):20-28.
- Newman KB. 2003. Modelling paired release-recovery data in the presence of survival and capture heterogeneity with application to marked juvenile salmon. *Statistical Modelling* 3(3):157-177.
- Newman KB, Rice J. 2002. Modeling the survival of Chinook salmon smolts outmigrating through the lower Sacramento River system. *Journal of the American Statistical Association* 97(460):983-993.
- Nobriga ML, Feyrer F, Baxter RD, Chotkowski M. 2005. Fish community ecology in an altered river Delta: Spatial patterns in species composition, life history strategies, and biomass. *Estuaries* 28(5):776-785.
- Nobriga ML, Matica Z, Hymanson ZP. 2004. Evaluating entrainment vulnerability to agricultural irrigation diversions: a comparison among open-water fishes. In: Feyrer F, Brown LR, Brown RL, Orsi JJ, editors. *Early life history of fishes in the San Francisco Estuary and watershed*. Bethesda (MD): American Fisheries Society. p 281-295.
- North EW, Hood RR, Chao S-Y, Sanford LP. 2005. The influence of episodic events on transport of striped bass eggs to the estuarine turbidity maximum nursery area. *Estuaries* 28(1):108-123.
- Oltmann RN. 1998. Indirect measurement of Delta outflow using ultrasonic velocity meters and comparison with mass-balance calculated outflow. *IEP Newsletter* [Internet]. 11(1):5-8. Available from: <http://iep.water.ca.gov/report/newsletter/>
- Peterson MS. 2003. A conceptual view of environment-habitat-production linkages in tidal river estuaries. *Reviews in Fisheries Science* 11(4):291-313.
- SJRGA (San Joaquin River Group Authority). 2006. 2005 annual technical report: San Joaquin River agreement. Report to the State Water Resources Control Board. Available from: <http://www.sjrg.org/technicalreport>.
- Sommer T, Harrell B, Nobriga M, Brown R, Moyle P, Kimmerer W, Schemel L. 2001. California's Yolo Bypass: evidence that flood control can be compatible with fisheries, wetlands, wildlife, and agriculture. *Fisheries* 26(8):6-16.
- Stevens DE, Kohlhorst DW, Miller LW, Kelley DW. 1985. The decline of striped bass in the Sacramento-San Joaquin Estuary, California. *Transactions of the American Fisheries Society* 114(1):12-30.
- Venables WN, Ripley BN. 2003. *Modern applied statistics with S-PLUS*, 4<sup>th</sup> ed. New York (NY): Springer-Verlag.
- Visser AW. 1997. Using random walk models to simulate the vertical distribution of particles in a turbulent water column. *Marine Ecology Progress Series* 158: 275-281.
- Vogel DA. 2004. Juvenile Chinook salmon radio-telemetry studies in the northern and central Sacramento-San Joaquin Delta, 2002-2003, Final Report. (Contract Report for CALFED, administered by the National Fish and Wildlife Foundation.) Red Bluff (CA): Natural Resource Scientists, Inc. 188 p.
- Wilbur R. 2000. Validation of dispersion using the particle tracking model in the Sacramento-San Joaquin Delta [master's thesis]. Davis (CA): University of California.
- Wilbur R. 2001. Validation of dispersion using the particle tracking model in the Sacramento-San Joaquin Delta. Chapter 4 in CDWR 2001.

## APPENDIX. EVALUATION OF THE CALIBRATION OF DSM2.

Although considerable effort has gone into calibrating, testing, and validating Delta Simulation Model 2 (DSM2), none of this work has been published. Here we compare DSM2 output with field data for stage, flow, and specific conductance. There are no data to calibrate DSM2–PTM directly. The PTM could be tested against the water quality module QUAL for cases of scalar release at several locations, but this has not been done. Thus, the results here should give an indication of how well the hydrodynamic module performs and how well mixing is represented, but there may still be issues with the translation to particle tracking that cause the PTM to be inaccurate.

*Stage and flow:* Model output and data on stage (elevation, m) and flow ( $\text{m}^3 \text{s}^{-1}$ ) at 15-minute intervals were obtained from the Department of Water Resources (C. Enright, pers. comm.). Plots using some of these data are available at <http://www.iep.ca.gov/dsm2pwt/calibrate/Run56vsRun1/index.html>. We selected April 1997 and April 1998 for comparisons because the data were complete for several stations in both time periods.

For each station, year, and variable, we adjusted the model data forward or back in time to obtain the highest correlation to determine how much the model led or lagged the field data. This was always < 1 hour. Regression analysis of the field data against the model gave a slope and correlation coefficient. Correlations, mean differences (data – model), and mean ratios (data:model) were calculated on data averaged by day. A good fit of the model to data would result in a correlation coefficient close to 1, a slope of 1, mean difference of 0, and mean ratio of 1.

In most cases, there was excellent agreement between the model and data (Table A1, example in Figure A1). Correlations of raw data were always close to 1, and correlations of daily-averaged data were almost all > 0.9. Slopes of the regressions (data on model) tended to be somewhat below 1 for stage, while slopes for flow were all between 0.9 and 1.1. Mean differences in stage were substantial in a few cases, notably Jersey Point and Three Mile Slough. Mean differences in flow were usually small in relation to daily means;

the largest mean difference (Jersey Point flow in 1998) was ~10% of the mean of the data. Amplitudes of the model output generally exceeded those of the data by up to 25% for stage, but were within 11% for flow.

Based on these results, the model appears to provide a simulation of stage and flow variability that reasonably represents the field observations. The most obvious deviation between model and data was for stage at two stations. This is probably due to errors in the datum for each of these tidal gages: if these were real errors, the representation of flow would be seriously in error. The other notable discrepancy is in tidal amplitude; the greater amplitude of stage in the model is not reflected in greater amplitude in flow, suggesting that frictional effects may be slightly exaggerated in the model. However, since our interest is in water movement, the accurate representation of flow patterns at all stations is encouraging.

*Salinity:* Model output has been framed in terms of specific conductance rather than salinity. Unlike salinity, specific conductance is not a conservative property and therefore not a clear indicator of mixing. Salinity is defined as a polynomial function of specific conductance that is slightly curved throughout its range. Furthermore, some salinity enters the Delta through agricultural runoff, so at low levels salinity is likewise ambiguous as a tracer of mixing. The result of these sources of uncertainty is that the use of specific conductance for calibrating the QUAL model is most reliable at higher values.

Output from the QUAL module was provided by the California Department of Water Resources (CDWR) as daily means for several nodes from 1990–2006. We downloaded data from the IEP website (<http://www.iep.ca.gov/dss/all/>) from five stations in Suisun Bay and the western Delta that matched QUAL nodes. One of these stations, Three Mile Slough, had an incomplete data record and was not used. The remaining stations had more than one reported value for some days. For example, the Mallard Slough (river kilometer 75) station included five different records, which were either “real-time” or “historical,” the former considered preliminary according to the website. Data were reported at different intervals (daily, hourly, or

**Table A1.** Summary of calibration data for DSM2 for April 1997 and April 1998. Lag is the number of minutes (15-minute increments) the model output had to be advanced to provide the best fit to the data. The slopes are for  $x =$  lagged model data and  $y =$  observed; 95% confidence limits determined after sampling the data-set to eliminate auto-correlation were 0.02 to 0.04. The daily correlation is based on applying a Godin low-pass filter to remove tidal signals and averaging the data by day, then determining the correlation. The mean difference is data - model, and the amplitude ratio is the mean of the ratio of daily amplitudes in the data to those in the model.

Location	Year	Lag (min)	Correlation	Slope	Daily Correlation	Mean Diff	Amplitude Ratio
<b>Stage (m)</b>							
Jersey Point	1997	0	0.99	0.94	0.95	0.27	0.94
Jersey Point	1998	0	0.99	0.91	0.99	0.25	0.89
Old River	1997	30	0.99	0.84	0.91	0.00	0.85
Old River	1998	15	0.99	0.80	0.98	0.02	0.80
Middle River	1997	30	0.99	0.83	0.90	0.06	0.85
Middle River	1998	15	0.99	0.81	0.99	0.03	0.80
Dutch Slough	1997	-15	0.99	0.97	0.93	0.13	0.97
Dutch Slough	1998	-15	0.99	0.93	0.98	0.05	0.94
Sac. R. above DCC	1997	15	0.98	0.82	0.91	0.01	0.83
Sac. R. above DCC	1998	15	1.00	1.05	1.00	-0.08	0.75
Three Mile Slough	1997	-15	0.99	0.95	0.94	0.18	0.95
Three Mile Slough	1998	-15	0.99	0.89	0.97	0.16	0.88
<b>Flow (<math>m^3 s^{-1}</math>)</b>							
Jersey Point	1997	15	1.00	0.91	0.95	3	0.91
Jersey Point	1998	15	1.00	0.90	0.92	105	0.93
Old River	1997	0	0.99	1.08	0.95	8	1.05
Old River	1998	15	1.00	1.05	0.97	-9	1.04
Middle River	1997	30	0.99	0.98	0.95	8	1.00
Middle River	1998	45	0.99	0.94	0.99	-4	0.98
Dutch Slough	1997	15	0.99	0.98	0.83	3	0.94
Dutch Slough	1998	30	0.99	0.94	0.94	11	0.91
Sac. R. above DCC	1997	45	0.99	1.06	0.99	-14	1.11
Sac. R. above DCC	1998	0	1.00	0.94	1.00	7	1.03
Three Mile Slough	1997	15	0.99	1.02	0.95	-6	1.06
Three Mile Slough	1998	30	0.99	0.94	0.97	-2	0.97



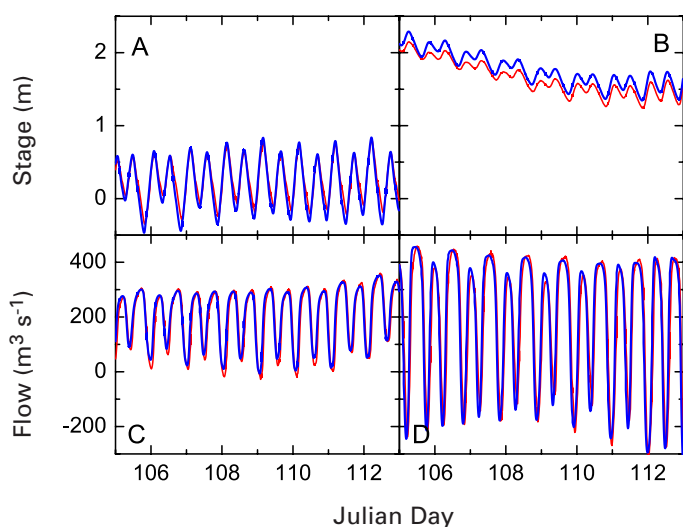


**Figure A1.** Examples of comparison of DSM2 model output (blue) with data (red) from USGS flow-measuring stations, including comparisons with largest time lags and poorest fits. A, B, stage; C, D, flow. A, C, starting date 15 April 1997; B, D, starting date 15 April 1998. A, D, Middle River near DSM2 Node 124; B, C, Sacramento River above the Delta Cross Channel (near Node 341).

every 15 minutes) and from different sources (CDWR, California Data Exchange Center, or U.S. Bureau of Reclamation). Some data were identified as having come from a bottom sensor. Nearly all of these data sources overlapped each other to some degree, and none had a complete record. We selected 2002–2006 for analysis because data were more complete than from other times.

To derive a consensus value for specific conductance at each station on each date, we simply took the medians of all the data for each date. This approach results in some error due to the limited availability of data from the bottom sensors. However, stratification in this part of the estuary is weak most of the time, and inspection of the data showed that field data from different sources were more similar to each other than to the model output. Once medians were calculated, there remained some missing values for all of the stations. These were filled in for each station by first determining which other station was most closely correlated with it, then constructing a generalized additive model with loess smoother (since we had no expectation about the form of the rela-

tionship) and filling in gaps by prediction. From the four stations with 1,827 records each, a total of 220 data points were filled by prediction, and six remaining gaps were filled by interpolation. This gave a complete 5-year record of specific conductance to compare with the model output. This comparison was made by linear regression and also by examining medians and 10th and 90th percentiles of the difference between data and model, and the percent difference.

The comparison of the model with data was generally good (Figure A2). The model tracked the summer high-salinity periods well. Scatter-plots (Figure A3) show how scatter increased with distance from the ocean, and with salinity. These increasing errors reflect, in part, the relatively low values of specific conductance; the possible influence of agricultural runoff at the more landward stations; and, in some cases, obvious spikes in the data that suggest the data are unreliable at those points. In some cases,

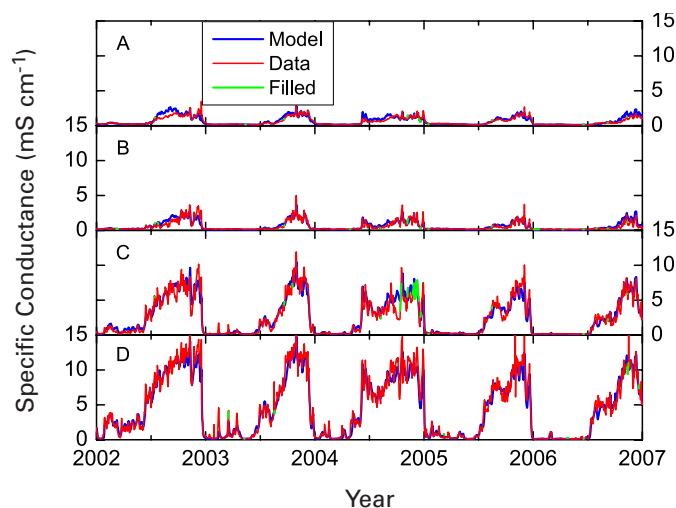


**Figure A2.** Time series of model output with measured data for specific conductance at 4 stations in 2004–2006. Model results are complete for the entire time period; measured results are complete except where filled by green lines. Note the difference in scales among stations; maxima in the four panels in terms of salinity (practical salinity scale) are 12, 9, 2.1, and 1.6. Stations are on the Sacramento River at: A, Chipps Island (river kilometer 75); B, Collinsville (river kilometer 81); C, Emmaton (river kilometer 92, halfway between Collinsville and Rio Vista); and D, on the San Joaquin River at Jersey Point (river kilometer 18, ~99 km from the mouth of the estuary).



**Table A2.** Summary of calibration data for DSM2 QUAL, daily data for 2002–2006. Locations are shown on Figure 1 except for Emmaton, which is at river kilometer 92, between Collinsville and Rio Vista. Median difference and percent difference are data - model.

Location	Correlation	Intercept	Slope ± CL	Median with 10th and 90th percentiles	
				Difference	Percent difference
Chippis Island	0.98	20	1.02 ± 0.07	25 (-777 – 1373)	4 (-26 – 49)
Collinsville	0.96	9	0.97 ± 0.10	6 (-808 – 742)	1 (-39 – 39)
Emmaton	0.89	30	0.85 ± 0.18	7 (-403 – 98)	4 (-40 – 29)
Jersey Point	0.91	48	0.83 ± 0.13	7 (-376 – 109)	3 (-32 – 27)

noticeable deviation of the model from the data occurred over a span of time (e.g., at Jersey Point early in summers, Figure A2A). These deviations were more noticeable in drier years (not shown), and could reflect uncertainty in the estimates of Delta outflow and particularly San Joaquin River flow during these periods. These flows are estimated from a water balance that relies on very uncertain estimates of net water consumption in the Delta (<http://www.iep.ca.gov/dayflow/documentation/>).

Consistent with the above observations, the statistical properties of the comparisons declined going from Chippis Island landward to Jersey Point (Table A2; correlation coefficients declined and slopes became flatter). However, the percentage differences between modeled and measured data did not vary much among sites.

These results also support the use of the DSM2 family of models for our particle-tracking work. The good correspondence between model and data in specific conductance means that the model is getting the salt balance about right, implying that longitudinal mixing is reasonably well-depicted. Furthermore, the close correspondence of model output and flow data, particularly the small mean differences in net flow in Table A1, imply that the model depicts net transport with reasonable accuracy.

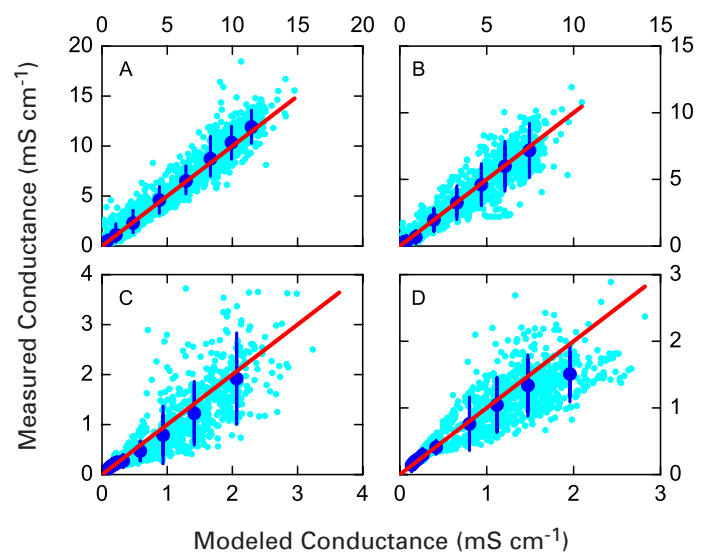


**Figure A3.** Data in Figure A2 as scatter-plots. Small circles, daily comparisons. Error bars, means with 10th and 90th percentiles of the data binned into 10 equal-size classes of model output and plotted against the model means by class. Straight line, 1:1 line.